

## Local Magnetic Relaxation in High-Temperature Superconductors

Y. Abulafia, A. Shaulov, Y. Wolfus, R. Prozorov, L. Burlachkov, and Y. Yeshurun

*Department of Physics, Bar-Ilan University, Ramat-Gan 52900, Israel*

D. Majer and E. Zeldov

*Department of Condensed Matter Physics, The Weizmann Institute of Science, Rehovot 76100, Israel*

V. M. Vinokur

*Materials Science Division, Argonne National Laboratory, Argonne, Illinois 60439*

(Received 14 March 1995)

A novel Hall probe array technique is used to measure the spatial distribution and time dependence of the magnetic induction in  $\text{YBa}_2\text{Cu}_3\text{O}_{7-\delta}$  crystals. Analysis of the data based on the flux diffusion equation allows a direct, model-independent determination of the *local* activation energy  $U$  and the logarithmic time scale  $t_0$  for flux creep. The results indicate that the spatial variations of  $U$  are small ( $\pm kT$ ) and that  $U$  increases logarithmically with time. The time  $t_0$  is inversely proportional to the field and it exhibits a nonmonotonic temperature dependence. These results confirm theoretical predictions based on the logarithmic solution of the flux diffusion equation.

PACS numbers: 74.60.Ge, 74.72.-h

Thermally activated flux creep in high-temperature superconductors is a subject of intensive study. This phenomenon is commonly investigated by measuring the time dependence of the magnetic moment  $M$  averaged over the sample volume. Among the most significant parameters extracted from such data are the effective activation energy  $U$  and the logarithmic time scale  $t_0$  for flux creep [1]. Recent models emphasize the nonlinear dependence of  $U$  on the current density  $j$  [2,3] and the macroscopic nature of the time scale  $t_0$  [1-6]. While it is not possible to derive  $U(j)$  directly from the experimental data, each of the above models gives a specific relaxation behavior that can be compared with experimental results. Such an approach for evaluating  $U(j)$  is model dependent and involves fitting several parameters [7].

Maley *et al.* [8] proposed a method to determine  $U(j)$  avoiding the *a priori* assumption of a model for the dependence of  $U$  on the current density and field. Their method analyzes global magnetic relaxation data, utilizing an integrated form of the flux diffusion equation over the sample volume. It is important to realize that the activation energy determined by this method is actually the activation energy *at the surface* of the sample, while the current density  $j$  is averaged over the sample volume [9]. Although in the limit  $U/kT \gg 1$  the activation energy should be almost constant over the sample volume [1,4], in the presence of surface barriers [10-12] the values of  $U$  at the surface and in the bulk may be different.

In this work we propose a method to determine the *local*  $U$  and  $j$  *in the bulk*, utilizing the recent development of a miniature Hall probe array [12] to measure the local induction  $B$  at different locations *simultaneously* as a function of time. In contrast with the conventional techniques where only the time evolution of the total

magnetization is recorded, we measure the time evolution of the spatial distribution of  $B$ , and thus are able to determine both the *time* and the *spatial derivatives* of  $B$ . This new information enables direct analysis of the local relaxation data using the basic diffusion equation governing the flux motion [4,13]:

$$\frac{\partial B}{\partial t} = -\nabla \cdot \mathbf{D}, \quad (1)$$

where  $\mathbf{D} = B\mathbf{v}$  is the flux current density and  $\mathbf{v} = v_0 \exp(-U/kT)$  is the effective vortex velocity. The preexponential factor  $v_0 = \mathcal{A}j\phi_0/c\eta$ , where  $\phi_0$  is the unit flux,  $c$  is the light velocity,  $j$  is the current density,  $\eta$  is the viscosity coefficient, and  $\mathcal{A}$  is a numerical factor [4]. In the slab geometry, where all the quantities depend on a single coordinate  $x$ ,  $j = -(c/4\pi)\partial B/\partial x$  and

$$\frac{\partial B}{\partial t} = -\frac{\partial D}{\partial x}; \quad D = \frac{\mathcal{A}\phi_0}{4\pi\eta} B \frac{\partial B}{\partial x} e^{-U/kT}. \quad (2)$$

The basic idea of our approach is to use the Hall probe array for simultaneous measurements of  $B$ ,  $\partial B/\partial x$  and  $\partial B/\partial t$ , that appear in Eq. (2). As described below, this allows measurements of  $U$  directly without assuming any specific model regarding the flux creep mechanism.

Measurements were performed on two single crystals of  $\text{YBa}_2\text{Cu}_3\text{O}_7$  [14,15] having a transition temperature  $T_c \approx 91$  K and a transition width of less than 0.5 K as deduced from dc measurements at 1 Oe. The crystals were cut into rectangular shape of sizes  $0.45 \times 0.23 \times 0.1$  mm<sup>3</sup> and  $1.2 \times 0.5 \times 0.2$  mm<sup>3</sup> (samples Y1 and Y2, respectively). The Hall probes were made of GaAs/AlGaAs 2DEG. An array of 11 elements, with  $10 \times 10$   $\mu\text{m}^2$  active area and sensitivity better than 0.1 G, was in direct contact with the surface of the crystal, as sketched in the inset of Fig. 1. The crystal and the probes were placed on a temperature-controlled sample holder inside a coil providing a dc field

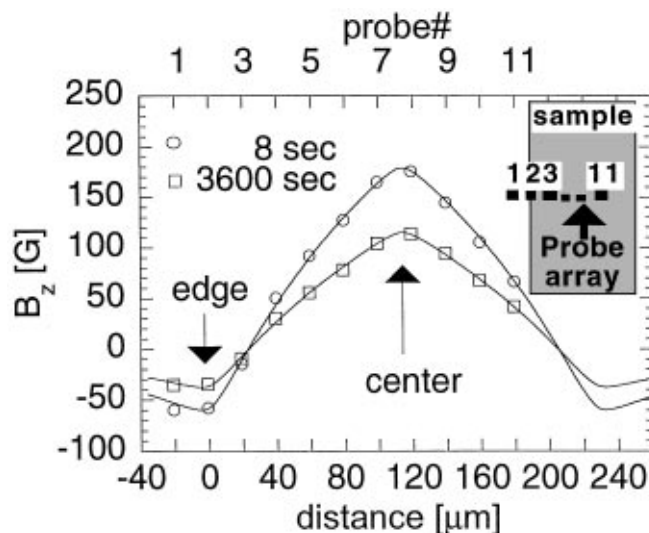


FIG. 1. Local induction  $B_z$  vs Hall probe location measured in crystal Y1 at  $T = 50$  K, 8 s and 1 h after removal of the external field. The solid lines, which are a result of model calculations, serve here only as a guide for the eye. Inset: Configuration of Hall probe array related to the crystal.

parallel to the  $c$  axis of the crystal. The probes detect the component  $B_z$  of the field normal to the surface of the crystal.

The experiment was carried out as follows. After zero-field cooling the sample from above  $T_c$ , we measured the profile  $B_z(x)$  for various applied fields  $H_a$ , on the ascending and descending branches of  $B_z(H)$ . This enabled visual verification of the establishment of a “critical state” which is essential for the flux creep experiments. Once a critical state was established, the field profile was measured every 13 s for a period of 1 h.

Figure 1 displays a typical field profile  $B_z(x)$  across the sample width  $d = 230 \mu\text{m}$  measured in a remanent state at 50 K, for crystal Y1. The solid line in the figure, which serves only as a guide for the eye, was calculated by using a Kim-like model for a platelet sample in a perpendicular field. The profiles of Fig. 1 show signatures of demagnetization effects typical for such samples [16–18], e.g., a sign reversal of  $B_z$  near the edge, approximately at the location of probe 3 at  $x_0 \approx 0.1d$ . In such samples, the relation  $j = -(c/4\pi)\partial B_z/\partial x$  used in Eq. (2) should be replaced by  $j = -(c/4\pi)(\partial B_z/\partial x - \partial B_x/\partial z)$ . However, numerical simulations show that in our samples, for which the ratio (thickness)/(width)  $\approx 0.5$ ,  $j$  can be approximated by  $f(x)(c/4\pi)(\partial B_z/\partial x)$ , where the correction factor  $f(x) \approx 0.8$  throughout most of the sample, except for regions near the center and the edges. Taking this correction into account in the evaluation of  $j$  had only a small effect ( $< 10\%$ ) on the results.

Figure 2 shows  $B_z$  as a function of time at different locations in the sample. Evidently, the relaxation rate

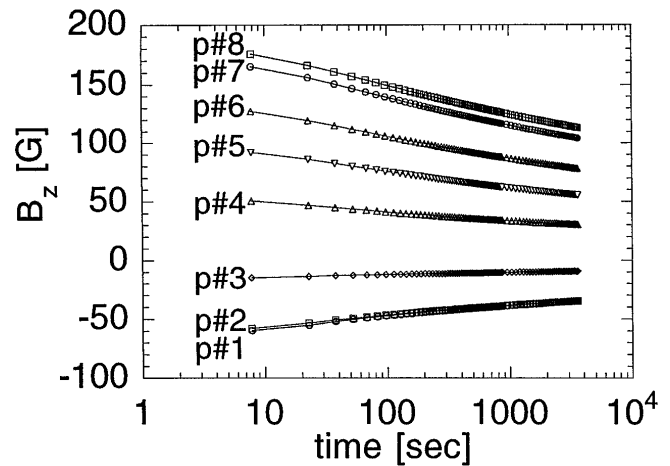


FIG. 2.  $B_z$  vs time measured at different locations in and out of the crystal.

$\partial B_z/\partial(\ln t)$  is maximum near the center and decreases toward the edge. Probe 3, located near the point  $x_0 \approx 0.1d$  where  $B_z \approx 0$ , shows approximately zero relaxation rate. The point  $x_0$  corresponds to a contour where vortices of different sign annihilate. As a direct consequence of the sign reversal of  $B_z$  near the edge, the induction at the sample edge *increases* with time, exhibiting a *positive* relaxation rate. This result emphasizes the nonuniformity of the local relaxation, thus questioning the meaning of global measurements in which negative and positive contributions are combined.

Using the raw  $B_z(x, t)$  data, we calculate the local relaxation rates  $\partial B_z(x, t)/\partial t$ , and then numerically integrate  $\partial B_z(x, t)/\partial t$  in order to determine the flux current density  $D(x, t)$  according to Eq. (2):

$$D(x, t) = - \int_{d/2}^x \frac{\partial B_z(x, t)}{\partial t} dx. \quad (3)$$

In Eq. (3)  $x = d/2$  is the center of the sample where  $D \equiv 0$ . Knowing  $D(x, t)$ , we obtain the *local* activation energy  $U(x, t)$ , using Eq. (2):

$$\frac{U(x, t)}{kT} = - \ln \left( \frac{4\pi\eta D}{\mathcal{A}\phi_0 B_z(\partial B_z/\partial x)} \right). \quad (4)$$

We take the flux viscosity coefficient  $\eta(T)$  from Ref. [19] and assume  $\mathcal{A} = 1$ , as will be justified below. Typical results of  $U/kT$  at 40 K are shown in Fig. 3 as a function of time. The figure shows a linear dependence of  $U/kT$  on  $\ln(t)$  with a slope of 1 in the long-time limit. This is in accordance with the general solution of the diffusion equation (2) with logarithmic accuracy [20,21]:

$$U = kT \ln(t/t_0) \quad (5)$$

with [1,4]

$$t_0 = \frac{\pi}{2} \frac{kT\eta d^2}{\mathcal{A}\phi_0 |\partial U/\partial j| j B_z(0)}, \quad (6)$$

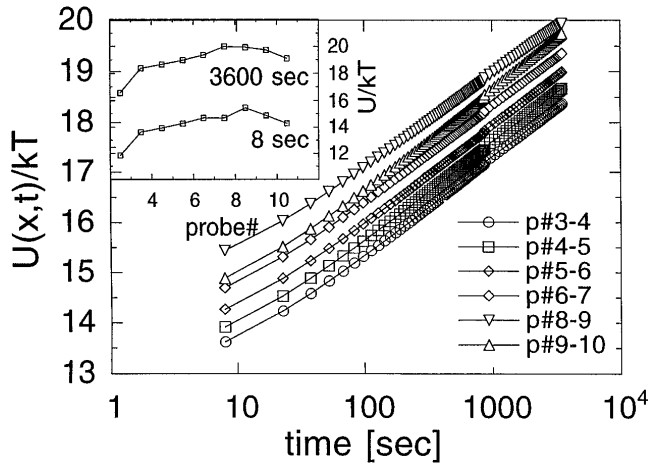


FIG. 3. Local activation energy  $U/kT$  vs time for different probes at  $T = 40$  K. For all the probes Eq. (5) holds perfectly.  $U$  is almost constant throughout the sample as shown in the inset.

where  $B_z(0)$  is the magnetic induction at the sample edge. The inset of Fig. 3 demonstrates that  $U$  is almost constant (within  $\pm kT$ ) throughout the sample. This is consistent with the predictions of models based on the concept of self-organized criticality [1,4].

In Fig. 4 the activation energy  $U/kT$ , calculated as an average between probes 5 and 6, is plotted as a function of  $j$ . This location is approximately in the middle between the sample edge and the center, where the difference between  $j$  and  $(c/4\pi)\partial B_z/\partial x$  is negligible. Evidently, the isothermal segments in Fig. 4 do not describe a continuous curve, reflecting a strong dependence of  $U$  on temperature. The best fit for each isotherm was obtained using the expression [3]

$$U = U_c \ln(j_c/j). \quad (7)$$

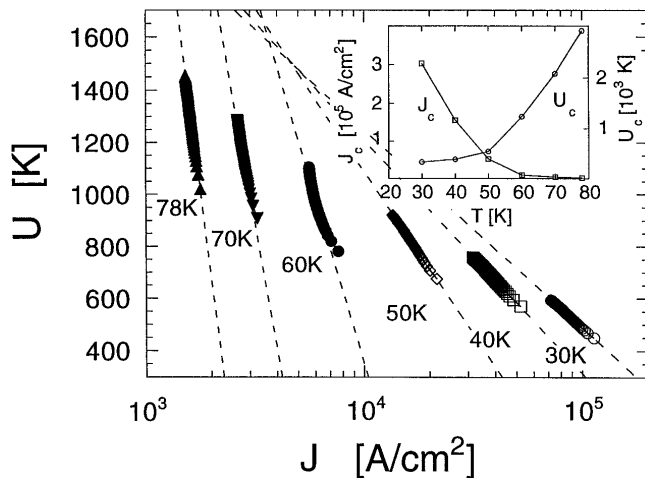


FIG. 4. Activation energy  $U$  vs  $j$  at different temperatures. The lines correspond to the fit:  $U = U_c \ln(j_c/j)$ . The dependence of  $U_c$  and  $j_c$  on temperature is shown in the inset.

Plots of  $U_c(T)$  and  $j_c(T)$  obtained from these fits are shown in the inset of Fig. 4. In the collective, as well as in the single vortex pinning regimes, one expects [1]  $U_c \approx \text{const}$  for  $T < T_{dp}$ , where  $T_{dp}$  is the depinning temperature. From Fig. 4 we estimate  $T_{dp} \approx 55$  K. Above  $T_{dp}$  the data of Fig. 4 exhibit an almost linear increase of  $U_c$  with  $T$ . This is typical for the single vortex pinning, whereas for collective pinning  $U_c$  grows with temperature more rapidly [1].

We turn now to discuss the behavior of the logarithmic time scale  $t_0$ . As noted by Feigel'man *et al.* [2,4],  $t_0$  is a macroscopic quantity depending on the sample size  $d$  [see Eq. (6)]; it is, however, related to the microscopic attempt frequency  $\omega$  and the hopping distance  $l$  through the velocity  $v_0 = \mathcal{A}j\phi_0/c\eta \propto \omega l$ . From Eq. (5) one can find  $t_0$  by extrapolating the data of Fig. 3 to  $U = 0$ . The circles in Fig. 5 show the temperature dependence of  $t_0$  for crystal Y1 for the case of remanent relaxation. At low temperatures ( $T < T_{dp}$ )  $t_0$  increases with  $T$  then exhibits a broad maximum between 60 and 75 K and finally drops as  $T$  approaches  $T_c$ . This behavior can be compared with the prediction of Eq. (6) by substituting  $U_c/j$  for  $|\partial U/\partial j|$  [see Eq. (7)], and  $B_z(0) \approx (4\pi/c)j_c x_0$ . All the parameters in Eq. (6) are now experimentally known. The squares in Fig. 5 are results of calculation of  $t_0$ , using Eq. (6) and taking  $\mathcal{A} \approx 1.4$  to obtain the best fit to the directly measured values of  $t_0$ . Evidently, the calculated and measured values of  $t_0$  exhibit similar behavior. It is worth noting that the result  $\mathcal{A} \approx 1.4$  justifies the neglect of  $\ln \mathcal{A}$  in Eq. (4) for  $U/kT \approx 15$ .

We also tested the validity of Eq. (6) for the dependence of  $t_0$  on  $H_a$  and on the size of the sample. For this purpose we measured  $B_z(x, t)$  in the larger sample (Y2) in the presence of a field and in the remanent state. The results shown in the inset of Fig. 5, for 78 K, were also

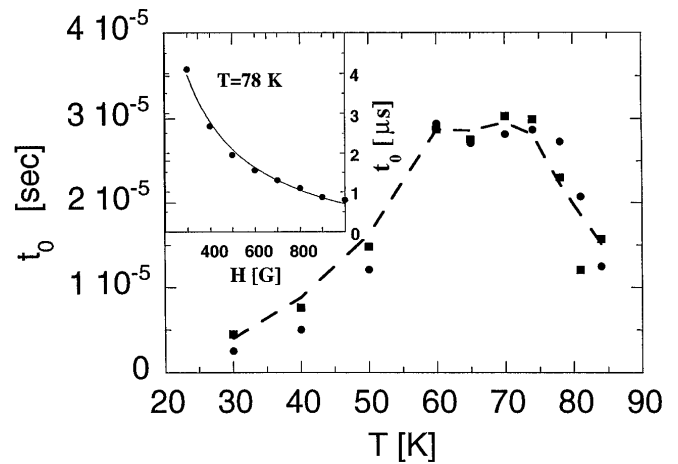


FIG. 5. Measured (circles) and calculated (squares) values of the logarithmic time scale  $t_0$  vs temperature for sample Y1. The dashed line is a guide for the eye for the calculated points. Inset: Field dependence of  $t_0$  for sample Y2. The solid line is proportional to  $1/H_a$ .

obtained directly by extrapolating the  $U$  vs  $\ln(t)$  data to  $U = 0$ . These results demonstrate that  $t_0$  decreases inversely with the field in accordance with the theoretical prediction [see Eq. (6)] described by the solid line in the figure. The value of  $t_0$  deduced from the remanent relaxation in the large sample Y2 (not shown in the figure) is  $10^{-4}$  s, larger by a factor of  $\approx 3.5$  than the value obtained in Y1 at the same temperature, in good agreement with the prediction of the size dependence in Eq. (6).

In conclusion, we have demonstrated a new technique for determining the activation energy  $U$  and the logarithmic time scale  $t_0$ . The method employs an array of Hall probes to measure the time evolution of the field profile in the sample, thus enabling direct analysis of the flux creep on the basis of the flux diffusion equation. This unique method allows determination of the *local* activation energy  $U(x, t)$  without engaging any specific model concerning the  $U(j, B)$  dependence. Using this technique, we obtained, for the first time, the logarithmic time scale  $t_0$  as a function of temperature, field, and sample size. The results confirm theoretical predictions based on the general solution of the flux diffusion equation with a logarithmic accuracy.

We are grateful to F. Holtzberg, M. Konczykowski, A. Erb, and H. Wuhl for providing the crystals for this study. We thank H. Shtrikman for growing the GaAs heterostructures, and acknowledge useful discussions with M. Konczykowski, P. Kes, V.B. Geshkenbein, and N. Wisser. This work was supported by the DG XII, Commission of the European Communities, by the Israeli Ministry of Science and the Arts, by the German-Israel Foundation (G.I.F.), and by the France-Israel cooperation program AFIRST. V.M.V. acknowledges support from the U.S. Department of Energy, BES-Material Sciences, under Contract No. W-31-109-ENG-38.

---

[1] G. Blatter, M. V. Feigel'man, V.B. Geshkenbein, A.I. Larkin, and V.M. Vinokur, *Rev. Mod. Phys.* **66**, 1125 (1994).

- [2] M. V. Feigel'man, V.B. Geshkenbein, A.I. Larkin, and V.M. Vinokur, *Phys. Rev. Lett.* **63**, 2303 (1989).
- [3] E. Zeldov, N.M. Amer, G. Koren, A. Gupta, R.J. Gambino, and M.W. McElfresh, *Phys. Rev. Lett.* **62**, 3093 (1989); *Appl. Phys. Lett.* **56**, 680 (1990).
- [4] M. V. Feigel'man, V.B. Geshkenbein, and V.M. Vinokur, *Phys. Rev. B* **43**, 6263 (1991).
- [5] M. Konczykowski, A.P. Malozemoff, and F. Holtzberg, *Physica (Amsterdam)* **185-189C**, 2203 (1991).
- [6] D.A. Brawner, N.P. Ong, and Z.Z. Wang, *Phys. Rev B* **47**, 1156 (1993).
- [7] J.R. Thompson, Yang Ren Sun, and F. Holtzberg, *Phys. Rev. B* **44**, 458 (1991).
- [8] M.P. Maley, J.O. Willis, H. Lessure, and M.E. McHenry, *Phys. Rev. B* **42**, 2639 (1990).
- [9] C.J. van der Beek, G.J. Nieuwenhuys, P.H. Kes, H.G. Schnack, and R. Griessen, *Physica (Amsterdam)* **197C**, 320 (1992).
- [10] L. Burlachkov, *Phys. Rev. B* **47**, 8056 (1993), and references therein.
- [11] Th. Schuster, M. V. Indenbom, H. Kuhn, E.H. Brandt, and M. Konczykowski, *Phys. Rev. Lett.* **73**, 1424 (1994).
- [12] E. Zeldov, A.I. Larkin, V.B. Geshkenbein, M. Konczykowski, D. Majer, B. Khaykovich, V.M. Vinokur, and H. Shtrikman, *Phys. Rev. Lett.* **73**, 1428 (1994).
- [13] M.R. Beasley, R. Labusch, and W.W. Webb, *Phys. Rev.* **181**, 682 (1969).
- [14] F. Holtzberg and C. Feild, *J. Cryst. Growth* **99**, 915 (1990).
- [15] A. Erb, T. Traulsen, and G. Muller-Vogt, *J. Cryst. Growth* **137**, 487 (1994).
- [16] David J. Frankel, *J. Appl. Phys.* **50**, 5402 (1979); M. Daumling and D.C. Larbalestier, *Phys. Rev. B* **40**, 9350 (1989).
- [17] E.H. Brandt, *Phys. Rev. B* **49**, 9024 (1994).
- [18] E. Zeldov, J.R. Clem, M. McElfresh, and M. Darwin, *Phys. Rev. B* **49**, 9802 (1994).
- [19] M. Golosovsky, M. Tsindlekht, H. Chayet, and D. Davidov, *Phys. Rev. B* **50**, 470 (1994).
- [20] L.B. Ioffe and V.M. Vinokur, *J. Phys. C* **20**, 6149 (1987).
- [21] V.B. Geshkenbein and A.I. Larkin, *Sov. Phys. JETP* **68**, 639 (1989).